We are IntechOpen,
the world's leading publisher of
Open Access books
Built by scientists, for scientists

6,900
Open access books available

186,000
International authors and editors

200M
Downloads

154
Countries delivered to

Our authors are among the

TOP 1%
most cited scientists

12.2%
Contributors from top 500 universities

CLARIVATE ANALYTICS
BOOK CITATION INDEX
INDEXED

WEB OF SCIENCE™

Selection of our books indexed in the Book Citation Index
in Web of Science™ Core Collection (BKCI)

Interested in publishing with us?
Contact book.department@intechopen.com

Numbers displayed above are based on latest data collected.
For more information visit www.intechopen.com

Chapter

Heat Exchanger Design and Optimization

Shahin Kharaji

Abstract

A heat exchanger is a unit operation used to transfer heat between two or more fluids at different temperatures. There are many different types of heat exchangers that are categorized based on different criteria, such as construction, flow arrangement, heat transfer mechanism, etc. Heat exchangers are optimized based on their applications. The most common criteria for optimization of heat exchangers are the minimum initial cost, minimum operation cost, maximum effectiveness, minimum pressure drop, minimum heat transfer area, minimum weight, or material. Using the data modeling, the optimization of a heat exchanger can be transformed into a constrained optimization problem and then solved by modern optimization algorithms. In this chapter, the thermal design and optimization of shell and tube heat exchangers are presented.

Keywords: log-mean temperature difference (LMTD), effectiveness-number of transfer units (ε-NTU), genetic algorithm (GA), particle swarm optimization (PSO)

1. Introduction

Heat exchangers are systems used to transfer heat between fluids with different temperatures. These devices have vast applications in many areas, such as refrigeration, heating, and air conditioning systems, power plants, chemical processes, food industry, automobile radiators, and waste heat recovery units. Heat exchangers can be classified according to different criteria such as construction, flow arrangement, heat transfer mechanism, etc [1]. The heat exchanger design can be divided into two main categories, thermal and hydraulic design and mechanical design. In thermal and hydraulic design, the focus is on calculating an adequate surface area transfer a certain amount of heat, pressure dope, pumping power work, etc. The goal of the mechanical design is to design the mechanical integrity of the exchanger, as well as designing various pressure and non-pressure components. In this chapter, the thermal and hydraulic design of heat exchangers is presented. To achieve better performance of heat exchangers, they optimize based on their application. Heat exchanger optimization can be performed using different optimization algorithms. Since most heat exchanger optimization problems are nonlinear, using traditional methods such as linear and dynamic programming and steepest descent may not lead to the desired solution and may even fail. Also, most traditional methods need gradient information to solve an optimization problem. On the other hand, advanced optimization algorithms are developed, which are gradient-free. Several

advanced optimization methods, such as genetic algorithm, non-nominated sorting genetic algorithm, bio-geography-based optimization, particle swarm optimization, Jaya algorithm, and teaching-learning-based optimization, can be more efficient in solving an optimization problem. However, each of these methods has its advantages and disadvantages, which are discussed in the optimization section. In this chapter, genetic algorithm and particle swarm optimization are discussed in detail due to the vast applications that arise from their acceptable accuracy, as well as short computational time [2].

2. Basic equation of heat transfer

In most heat transfer problems, hot and cold fluids are divided by a solid wall. In this case, the mechanism of heat transfer from hot fluid to the cold fluid can be categorized into three steps:

- Heat transfer from the hot fluid to the wall by convection.

- Heat transfer through the wall by conduction.

- Heat transfer from the wall to the cold fluid by convection.

Figure 1 shows a schematic of heat transfer between two fluids. As it can be seen, thermal resistance (R) is present at each stage of the transfer. Thermal resistance is a thermal (physical) property that indicates the resistance of each material to heat transfer due to temperature differences that can be calculated from [3]:

$$R = \frac{L}{KA} \text{ , for conduction}$$
$$R = \frac{1}{hA} \text{ , for convection}$$

(1)

Where L is the thickness of the wall, A is the cross-sectional area in which heat transfer occurs, and K and h are conduction and convection heat transfer coefficient, respectively.

Heat transfer in each stage can be calculated as follows [4]:

$$Q = \frac{T_1 - T_2}{R_{c,H}} = \frac{T_2 - T_3}{R_{f,H}} = \frac{T_3 - T_4}{R_w} = \frac{T_4 - T_5}{R_{f,C}} = \frac{T_5 - T_6}{R_{c,C}}$$

(2)

Where:
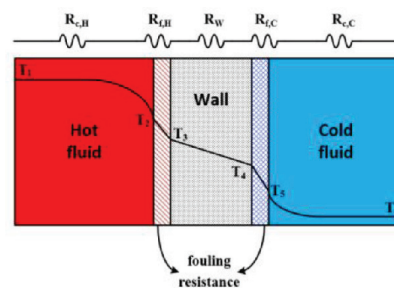$R_{c,H}$ = thermal resistance for convection in the hot side.

Figure 1.
A schematic of heat transfer in heat exchangers.

$R_{f,H}$ = fouling resistance of hot side.

R_w = wall resistance.

$R_{f,C}$ = fouling resistance of cold side.

$R_{c,C}$ = thermal resistance for convection in cold side.

Table 1 shows the fouling resistance of the most common fluids used in heat exchangers. The overall heat transfer coefficient can be obtained from Eq. (2) as follows [4]:

$$Q = \frac{T_1 - T_6}{R_{c,H} + R_{f,H} + R_w + R_{f,C} + R_{c,C}} \tag{3}$$

or:

$$Q = \frac{T_1 - T_6}{\frac{1}{h_H A_H} + \frac{r_{f,H}}{A_H} + \frac{r_w}{A_H} + \frac{r_{fC}}{A_C} + \frac{1}{h_C A_C}} \tag{4}$$

Gas and vapors	Fouling Factor $\left(\frac{hr-ft^2-{}^\circ F}{Btu}\right)$	Liquids		Fouling Factor $\left(\frac{hr-ft^2-{}^\circ F}{Btu}\right)$	
Industrial		**Industrial liquids**			
Manufactured Gas	0.01	Industrial organic heat transfer media		0.001	
Engine Exhaust Gas	0.01	Refrigerating liquids		0.001	
Steam (non-oil bearing)	0.0005	Molten heat transfer salts		0.0005	
Exhaust Steam (oil bearing)	0.001	Hydraulic fluid		0.001	
Refrigerant Vapors (oil bearing)	0.002	**Industrial oils**			
Compressed Air	0.002	Fuel oil		0.005	
Industrial Organic Heat Transfer Media	0.001	Engine lube oil		0.001	
Chemical Processing		Transformer oil		0.001	
Acid Gas	0.001	Quench oil		0.004	
Solvent Vapors	0.001	Vegetable oils		0.003	
Stable Overhead Product	0.001	**water**			
Petroleum Processing		Temperature of heating medium	240°F≤	240–400°F	
Atmospheric Tower Overhead Vapors	0.001	Temperature of water	125°F≤	125°F>	
Light Naphthas	0.001	velocity	3 ft.≤ 3 ft.>	3 ft. ≤ 3 ft. >	
Vacuum Overhead Vapors	0.002	Seawater	0.0005 0.0005	0.001 0.001	
Natural Gas	0.001	Brackish water	0.002 0.001	0.003 0.002	
Overhead Products	0.001	Distilled water	0.0005 0.0005	0.0005 0.0005	
Coke Unit Overhead Vapors	0.002	Boiler blowdown	0.002 0.002	0.002 0.002	

Table 1.
Fouling factors for different types of fluid [5, 6].

Where:

h_H and h_C = convection heat transfer coefficient of the hot and cold sides, respectively.

A_H and A_C = and surface area of wall in the hot and cold side, respectively.

The r_w can be calculated for flat wall and cylindrical walls using Eqs. (5) and (6), respectively.

$$r_w = \frac{d_w}{KA}, \; for \; flat \; wall \tag{5}$$

$$r_w = \frac{\ln\left(\frac{r_o}{r_i}\right)}{2\pi LK}, \; for \; cylindrical \; wall \tag{6}$$

Where d_w is the thickness of the wall, and r_o and r_i are the outside and inside diameter of the wall, respectively.

Total thermal resistance can be expressed as [7]:

$$R_t = \frac{1}{h_H A_H} + \frac{r_{f,H}}{A_H} + \frac{r_w}{A_H} + \frac{r_{f,C}}{A_C} + \frac{1}{h_C A_C} \tag{7}$$

The rate of heat transfer (Q) can be determined from

$$Q = UA\Delta T \tag{8}$$

Where U is the overall heat transfer coefficient.

$$U = \frac{1}{\frac{1}{h_H \frac{A_H}{A_{ref}}} + \frac{r_{f,H}}{\frac{A_H}{A_{ref}}} + \frac{r_w}{\frac{A_H}{A_{ref}}} + \frac{r_{f,C}}{\frac{A_C}{A_{ref}}} + \frac{1}{h_C \frac{A_C}{A_{ref}}}} \tag{9}$$

Where A_{ref} is a reference area. If the heat transfer is carried out over a pipe, the inside and outside surface areas of the pipe are not equal. Hence, the A_{ref} must be determined (The outer surface of the pipes is usually selected).

3. Thermal design of heat exchangers

The thermal design of heat exchangers can be performed by several methods. The most commonly used methods are log-mean temperature difference (LMTD) and effectiveness-number of transfer units (ε-NTU) [8]. The LMTD was used to calculate heat transfer when the inlet and outlet temperatures of fluids are specified. When more than one inlet and/or outlet temperature of the heat exchanger is unknown, LMTD may be calculated by trial and errors solution. In this case, the ε-NTU method is commonly used [3].

3.1 The log-mean temperature difference (LMTD) method

As mentioned earlier, by determining the temperature difference between hot and cold fluids, the amount of heat transfer can be calculated from Eq. (3). **Figure 2** shows temperature changes of hot and cold fluids along with a heat exchanger with different types of flow configuration. As it can be seen the temperature difference between hot and cold fluids can vary along with the heat exchanger. Terminal temperatures of hot and cold fluids ($T_{H,out}$ anf $T_{C,out}$) are very effective factors in a heat exchanger design. If $T_{C,out}$ is lower than $T_{H,out}$ for countercurrent flow,
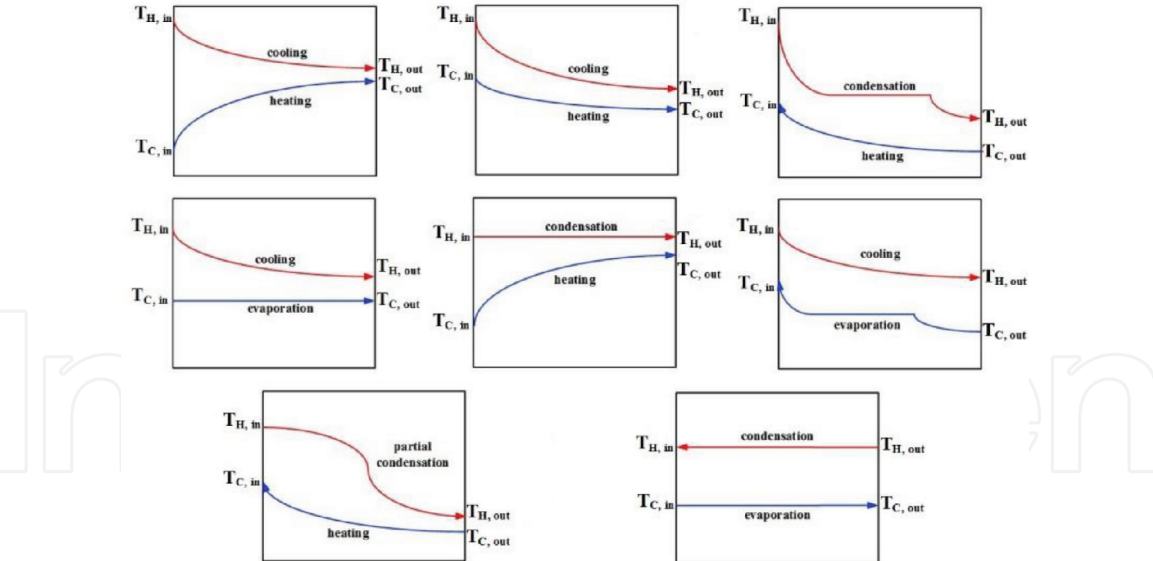
Figure 2.
Temperature changes of hot and cold fluids along with a heat exchanger with different types of flow configuration.

temperature approach occurs. In contrast, if $T_{C,out}$ is higher than the $T_{H,out}$ for countercurrent flow, temperature cross happens [9]. But if $T_{C,out}$ is equal to $T_{H,out}$, temperature meet takes place. Based on the second law of thermodynamics, temperature cross can never take place for heat exchangers with co-current flow configuration [10]. In 1981, Wales [11] proposed a parameter G, which can be used to determine the temperature conditions in the heat exchangers. Eq. (10) defines the G parameters that can be between −1 and 1.

$$G = \frac{T_{H,out} - T_{C,out}}{T_{H,in} - T_{C,in}},$$
$$G > 0 \rightarrow \quad temperature \ \ approach$$
$$G = 0 \rightarrow temperature \ \ meet \qquad\qquad (10)$$
$$G < 0 \rightarrow temperature \ \ cross$$

Since the temperature difference between hot and cold streams varies along with the heat exchanger, the basic question is which temperature difference should be considered to calculate the heat transfer rate. To answer this question, consider **Figure 3** which shows heat transfer between two parallel and co-current fluids. Based on **Figure 3**, the heat transfer for the specified heat transfer area can be written in the form:

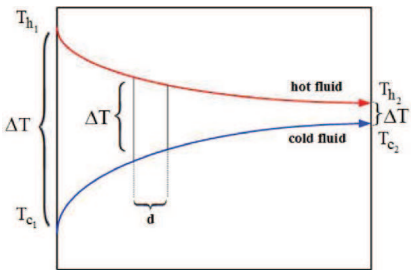$$dQ = U \ \Delta T \ dA \qquad\qquad (11)$$

Figure 3.
Heat transfer between two parallel and co-current fluids [3].

It can be said that the amount of heat transferred is reduced from the hot fluid and added to the cold fluid. Therefore [3]:

$$dQ = -C_{p,H} \, dT_H \tag{12}$$

$$dQ = C_{p,C} \, dT_C \tag{13}$$

Where $C_{p,H}$ and $C_{p,C}$ are specific heat capacities of hot and cold fluids, respectively. The temperature difference can be written as below:

$$d(\Delta T) = dT_H - dT_C \tag{14}$$

By the combination of Eqs. (12) and (13) with Eq. (14):

$$d(\Delta T) = -\frac{dQ}{C_{p,H}} - \frac{dQ}{C_{p,C}} \tag{15}$$

By defining $\frac{1}{M} = \frac{1}{C_{p,C}} + \frac{1}{C_{p,H}}$, Eq. (15) can be written as follow:

$$dQ = M \, d(\Delta T) \tag{16}$$

Assuming the M is constant along with the heat exchanger:

$$\int_0^Q dQ = -M \int_{\Delta T_{in}}^{\Delta T_{out}} d(\Delta T) \rightarrow Q = -M(\Delta T_{out} - \Delta T_{in}) \tag{17}$$

On the other hand, by placing Eq. (16) in Eq. (11):

$$-M\frac{d(\Delta T)}{\Delta T} = UdA = A\frac{UdA}{A} \tag{18}$$

$$A\int_0^A \frac{UdA}{A} = -M \int_{\Delta T_{in}}^{\Delta T_{out}} \frac{d(\Delta T)}{\Delta T} \rightarrow U_m A = -M \, \ln\left(\frac{\Delta T_{out}}{\Delta T_{in}}\right) \tag{19}$$

Where U_m is the mean overall heat transfer coefficient which can be defined as below:

$$U_m = \int_0^A \frac{U \, dA}{A} \tag{20}$$

The heat transfer rate can be written as flow:

$$Q = U_m A \Delta T_{LMTD} \tag{21}$$

Where ΔT_{LMTD} is the logarithmic mean temperature difference (LMTD) which can be defined as below:

$$\Delta T_{LMTD} = \frac{\Delta T_{out} - \Delta T_{in}}{\ln\left(\frac{\Delta T_{out}}{\Delta T_{in}}\right)} \tag{22}$$

The simplicity of the LMTD method has led to its use in the design of many heat exchangers by introducing a correction factor, F, according to Eq. (23) [12]. The F is generally expressed in terms of two non-dimensional parameters, thermal effectiveness (P), and heat capacity ratio (R). The P and R are defined as Eqs. (24) and (25), respectively [13]. **Figure 4** shows the correction factor for common shell and tube heat exchangers.

$$Q = UAF\Delta T_{LMTD} \ , \ \ 0 < F < 1 \tag{23}$$

$$P = \frac{T_{C,out} - T_{C,in}}{T_{H,in} - T_{C,in}} \tag{24}$$

$$R_{cr} = \frac{T_{H,in} - T_{H,out}}{T_{C,out} - T_{C,in}} \tag{25}$$

3.2 Effectiveness-number of transfer units (ε-NTU)

When more than one of the inlet and outlet temperatures of the heat exchanger is unknown, LMTD may be calculated by trial and errors solution. Another approach to calculating the rate of heat transfer is the effectiveness number of transfer units (ε-NTU) method. The ε-NTU can be expressed according to Eq. (26) where Cp_{min} is the minimum value between the heat capacity of cold fluid ($Cp_{,C}$) and hot fluid ($Cp_{,H}$). The effectiveness (ε) can be defined as the ratio of the actual heat transfer rate (q) and the maximum possible heat transfer rate (q_{max}) according to Eq. (27).

$$NTU = \frac{UA_m}{Cp_{min}} \tag{26}$$

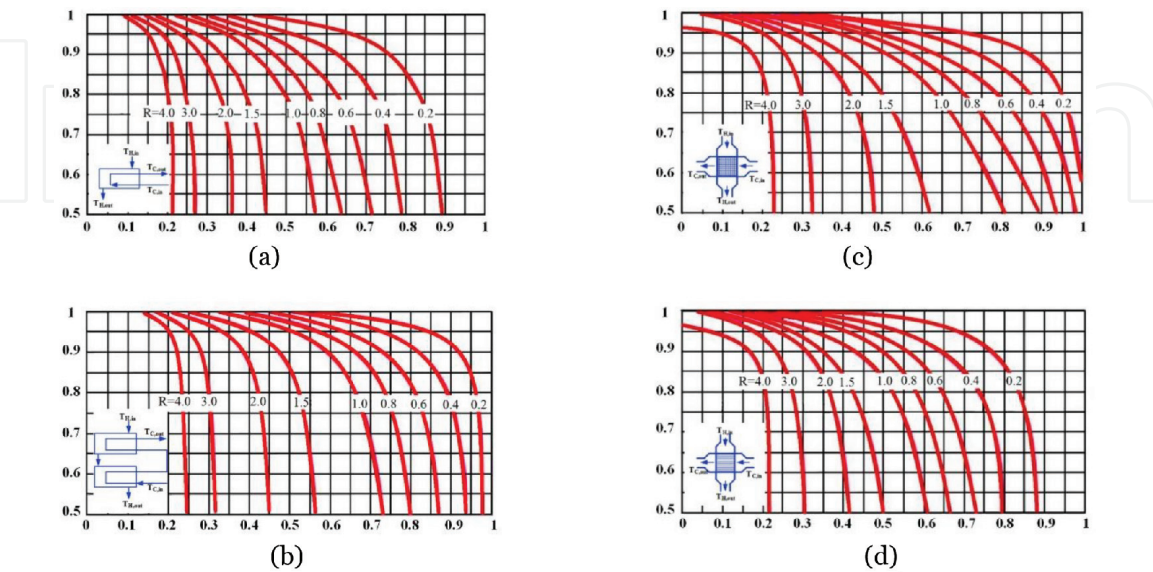$$\varepsilon = \frac{q}{q_{max}} \tag{27}$$

Figure 4.
Correction factor for common shell and tube heat exchangers [3]. (a) One-shell pass and 2, 4, 6, etc. (any multiple of 2), tube pass. (b) Two-shell pass and 4, 8, 12, etc. (any multiple of 4), tube pass. (c) Single-pass cross-flow with both fluids unmixed. (d) Single-pass cross-flow with one fluid unmixed and other unmixed.

Where:

$$q = Cp_{,H}(T_{H,in} - T_{H,out}) = Cp_{,C}(T_{C,out} - T_{C,in}) \qquad (28)$$

$$q_{\max} = C_{p\min}(T_{H,in} - T_{C,in}) \qquad (29)$$

The heat transfer rate using the ε-NTU method can express as [14]:

$$Q = \varepsilon C_{P\min}(T_{H,in} - T_{C,in}) \qquad (30)$$

Tables 2 and **3** show the effectiveness and NTU relations for heat exchangers, respectively. It should be noted that C_r is the capacity and it can be defined as follows:

$$C_r = \frac{C_{P\min}}{C_{P\max}} \qquad (31)$$

Heat exchanger type	Effectiveness relation
Double pipe: • Parallel-flow • Counter flow with $C_r < 1$ • Counter flow with $C_r = 1$	$\varepsilon = \frac{1 - \exp[-NTU(1+C_r)]}{1+C_r}$ $\varepsilon = \frac{1 - \exp[-NTU(1-C_r)]}{1 - C_r \exp[-NTU(1-C_r)]}$ $\varepsilon = \frac{NTU}{1+NTU}$
Sell and tube: • On-pass and 2, 4, … tube	$\varepsilon = 2\left\{ 1 + C_r + \sqrt{1+C_2}\, \frac{1 + \exp\left[-NTU\sqrt{1+C_2}\right]}{1 - \exp\left[-NTU\sqrt{1+C_2}\right]} \right\}^{-1}$
Cross flow (single-pass): • $C_{\max}$ and $C_{\min}$ unmixed • $C_{\max}$ mixed and $C_{\min}$ unmixed • $C_{\max}$ unmixed and $C_{\min}$ mixed	$\varepsilon = 1 - \exp\left[\frac{1}{C_r}(NTU)^{0.22}\left\{ \exp\left[-C_r(NTU)^{0.78} \right] - 1 \right\} \right]$ $\varepsilon = \frac{1}{C_r}\{1 - \exp[-C_r(1 - \exp[NTU])]\}$ $\varepsilon = 1 - \exp\left\{ -\frac{1}{C_r}(1 - \exp[-C_r NTU]) \right\}$
All heat exchangers with $C_r = 0$	$\varepsilon = 1 - \exp(-NTU)$

Table 2.
Effectiveness relation for heat exchangers [15].

Heat exchanger type	NTU relation
Double pipe: • Parallel-flow • Counter flow with $C_r < 1$ • Counter flow with $C_r = 1$	$NTU = -\frac{\ln[1 - \varepsilon(1+C_r)]}{1+C_r}$ $NTU = \frac{1}{C_r - 1}\ln\left(\frac{\varepsilon - 1}{\varepsilon C_r - 1} \right)$ $NTU = \frac{\varepsilon}{1-\varepsilon}$
Sell and tube: • On-pass and 2, 4, … tube	$NTU = -\frac{1}{\sqrt{1+C^2}}\ln\left[\frac{\frac{2}{\varepsilon} - 1 - C_r - \sqrt{1+C^2}}{\frac{2}{\varepsilon} - 1 - C_r + \sqrt{1+C^2}} \right]$
Cross flow (single-pass): • $C_{\max}$ mixed and $C_{\min}$ unmixed • $C_{\max}$ unmixed and $C_{\min}$ mixed	$NTU = -\ln\left[1 + \frac{\ln(1 - \varepsilon C_r)}{C_r} \right]$ $NTU = -\frac{\ln[C_r \ln(1-\varepsilon) + 1]}{C_r}$
All heat exchangers with $C_r = 0$	$NTU = -\ln[1 - \varepsilon]$

Table 3.
NTU relation for heat exchangers [15].

4. Thermal and hydraulic design of shell and tube heat exchanger

Heat exchangers can be classified according to different criteria such as construction, flow arrangement, heat transfer mechanism, etc [1]. Shell and tube heat exchangers are some of the most convenient heat exchangers due to their versatility, wide operating range, and simplicity [16]. Hence, this chapter focuses on the design of this type of heat exchanger. In the design of shell and tube heat exchangers, a lot of consideration including the number of shells and tubes, tube pitch and layout, tube passes, baffles, etc., should be taken into account. In this case, there are some methods such as Kern and Bell-Delaware to design a heat shell and tube exchanger design. Since Kern's method offers the simplest route, this chapter is focused on this method.

4.1 Kern's method

Kern's method is based on experimental data for typical heat exchangers. In this method, it is assumed the shell flow is ideal, and leakage and bypass are negligible. Based on this flow model, only a single stream flows in the shell that is driven by baffles. This can lead to a very simple and rapid calculation of shell-side coefficients as well as pressure drop [17]. **Figure 5** shows a schematic of a shell and tube heat exchanger.

4.2 Number of tubes

The number of tubes (N_t) can be calculated as follows:

$$N_t = \frac{4\,\dot{m}_t}{\rho_t \nu_t \pi d_i^2} \tag{32}$$

Where $\dot{m}_t$ is the flow rate of fluid inside the tube, ρ_t is the density of the fluid inside the tube, ν_t is the velocity of the fluid inside the tube, A_t is the cross-sectional area of the tube, and d_i is the tube inside diameter.

1. Shell
2. Shell cover
3. Shell flange (channel end)
4. Shell flange (cover end)
5. Shell nozzle or branch
6. Floating tube sheet
7. Floating head cover
8. Floating head flange
9. Floating head gland
10. Floating head backing ring
11. Stationary tube sheet
12. Channel or stationary head
13. Channel cover
14. Channel nozzle or branch
15. Tube (straight)
16. Tubes (U-type)
17. Tie rods and spacers
18. Transverse (or cross) baffles or support plates
19. Longitudinal baffles
20. Impingement baffles
21. Floating head support
22. Pass partition

Figure 5.
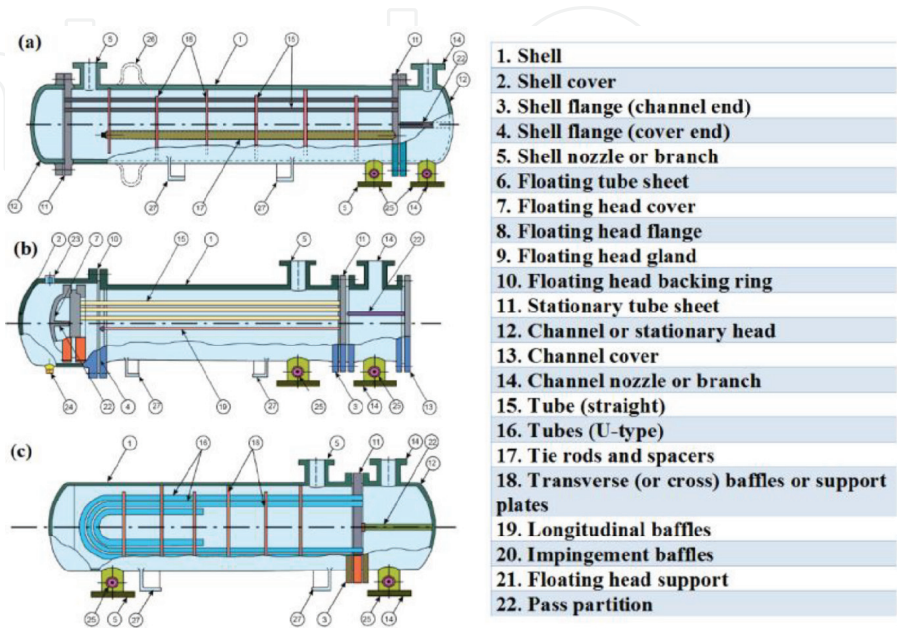*Schematic of a shell and tube heat exchanger a) fixed-tube b) floating-head c) removable U-tube [18].*

4.3 Tube-side heat transfer coefficient

The heat transfer coefficient for the tube side (h_t) is calculated as follows:

$$h_t = Nu_t \frac{k_t}{d_i} \tag{33}$$

Where Nu_t is the Nusselt number for the tube-side fluid and k_t is the thermal conductivity of the tube-side fluid. The Nu_t is a function of Reynolds number (Re) and Prandtl number (Pr). Re and Pr can be obtained by the following:

$$\text{Re}_t = \frac{\rho_t \nu_t d_t}{\mu_t} \tag{34}$$

$$\text{Pr}_t = \frac{C_p \mu_t}{K} \tag{35}$$

Where μ_t is the dynamic viscosity of the tube-side fluid, K is the heat conductivity coefficient, and C_p is the heat capacity of the tube-side fluid. The Nu_t can be calculated according to the type of flow as follows:

$$Nu_t = \frac{(f_t/2)\,\text{Re}_t \text{Pr}_t}{1.07 + 12.7(f_t/2)^{1/2}\left(\text{Pr}_t^{2/3} - 1\right)}; for: 10^4 < \text{Re} < 5 \times 10^6 \,\&\, 0.5 < \text{Pr} < 200 \tag{36}$$

$$Nu_t = 1.86\left(\frac{\text{Re}_t \text{Pr}_t d_i}{L}\right)^{1/3}; \quad for: \left(\frac{\text{Re}_t \text{Pr}_t d_i}{L}\right)^{1/3} > 2 \,\&\, 0.48 < \text{Pr} < 16700 \tag{37}$$

Where L is the length of the tube and f_t is the friction factor of the tube side, which can be calculated from

$$f_t = (1.58 \ln \text{Re}_t - 3.28)^{-2} \tag{38}$$

The convection heat transfer coefficient in the tube is obtained based on the value of the Re_t from [19]:

$$h_t = \frac{k_t}{d_i}\left[3.657 + \frac{0.0677\left(\text{Re}_t \text{Pr}_t \frac{d_i}{L}\right)^{1.3}}{1 + 0.1\text{Pr}_t\left(\text{Re}_t + \frac{d_i}{L}\right)^{0.3}}\right]; \; for \; \text{Re}_t < 2300 \tag{39}$$

$$h_t = \frac{k_t}{d_i}\left[\frac{\frac{\lambda}{8}(\text{Re}_t - 1000)\text{Pr}_t}{1 + 12.7\sqrt{\frac{\lambda}{8}}(\text{Pr}_t^{0.67} - 1)}\left(1 + \left(\frac{d_i}{L}\right)^{0.67}\right)\right]; \; for \; 2300 < \text{Re}_t < 10000 \tag{40}$$

$$h_t = \frac{k_t}{d_i} 0.027\,\text{Re}_t^{0.8}\text{Pr}_t^{\frac{1}{3}}\left(\frac{\mu_t}{\mu_{w,t}}\right)^{0.14}; \; for \; \text{Re}_t > 10000 \tag{41}$$

Where $\mu_{w,t}$ is the dynamic viscosity of the tube-side fluid at the wall temperature and λ is the Darcy friction coefficient which can be defined as [19]:

$$\lambda = (1.82 \log_{10} \log_{10} \text{Re}_t - 1.64)^2 \tag{42}$$

The tube-side pressure drop is calculated by the following:

$$\Delta P_t = \left(4f_t \frac{LN_p}{d_i} + 4N_p\right) \frac{\rho_t \mu_t^2}{2}$$ (43)

Where N_p is the tube passes.

4.4 Shell diameter

Inside sell diameter (D_s) is calculated as follows:

$$D_s = \sqrt{\frac{4AN_t}{(CTP)\pi}}$$ (44)

Where A is the projected area of the tube layout expressed as an area corresponding to one tube and can be obtained from Eq. (45). Also, P_t is tube pitch and CL is the tube layout constant. **Figure 6** depicts two common tube layouts, square pitch and triangular pitch. The CTP is the tube count calculation constant that accounts for the incomplete coverage of the shell diameter by the tubes, due to necessary clearances between the shell and the outer tube circle and tube omissions due to tube pass lanes for multitude pass design [15]. Eq. (46) shows the CTP for different tube passes.

$$\begin{aligned}
&A = P_t^2(CL) \\
&CL = 1 \rightarrow for\ square-pitch\ layout \\
&CL = 0.866 \rightarrow for\ triangular-pitch\ layout
\end{aligned}$$ (45)

$$\begin{aligned}
&CTP = 0.93 \rightarrow for\ one-tube\ pass \\
&CTP = 0.9 \rightarrow for\ two-tube\ pass \\
&CTP = 0.85 \rightarrow for\ three-tube\ pass
\end{aligned}$$ (46)

Combining Eq. (44) with Eq. (45) as well as defining tube pitch ratio as P_r, one gets:
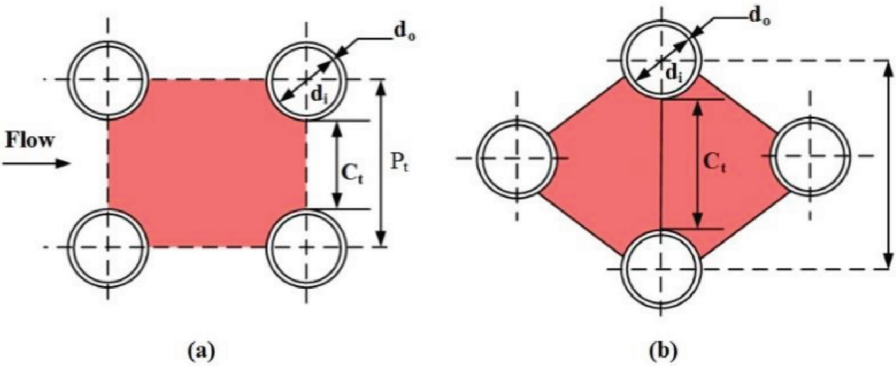
$$D_s = \sqrt{\frac{4(P_r d_o)^2(CL)N_t}{(CTP)\pi}}$$ (47)

Figure 6.
(a) Square-pitch (b) triangular-pitch layout [20].

$$P_r = \frac{P_t}{d_o} \tag{48}$$

Where d_o is tube outside the diameter. Eq. (47) can be written as follows:

$$D_s = \sqrt{\frac{4\left(P_r^2\right)(CL)A_o d_o}{(CTP)\pi^2 L}} \tag{49}$$

Where A_o is the outside heat transfer surface area based on the outside diameter of the tube and can be calculated from:

$$A_o = \pi d_o N_t L \tag{50}$$

The shell side flow direction is partially along the tube length and partially across to tube length or heat exchanger axis. The inside shell diameter can be obtained based on the cross-flow direction and the equivalent diameter (D_e) is calculated along the long axes of the shell. The equivalent diameter is given as follows:

$$D_e = \frac{4 \times free-flow\ area}{wetted\ perimeter} \tag{51}$$

From **Figure 6** the equivalent diameter for the square pitch and triangular pitch layouts are as below:

$$D_e = \frac{4\left(P_t^2 - \frac{\pi d_o^2}{4}\right)}{\pi d_o} \quad ;\ for\ square-pitch\ tube \tag{52}$$

$$D_e = \frac{4\left(\frac{P_t^2\sqrt{3}}{4} - \frac{\pi d_o^2}{8}\right)}{\frac{\pi d_o}{2}} \quad ;\ for\ triangular-pitch\ tube \tag{53}$$

Reynolds number for the shell-side (Re_s) can be obtained as follows:

$$\mathrm{Re}_s = \left(\frac{\dot{m}_s}{A_s}\right)\frac{D_e}{\mu_s} \tag{54}$$

Where $\dot{m}_s$ is the flow rate of shell-side fluid, μ_s is the viscosity of the shell-side fluid, and A_s is the cross-flow area at the shell diameter which can be obtained as below:

$$A_s = \frac{D_s}{P_t}(B \times C_t) \tag{55}$$

Where B is the baffle spacing and C_t is the clearance between adjacent tubes. According to **Figure 6** C_t is expressed as follows:

$$C_t = P_t - d_o \tag{56}$$

The shell-side mass flow rate (G_s) is found with:

$$G_s = \frac{\dot{m}_s}{A_s} \tag{57}$$

In Kern's method, the heat transfer coefficient for the shell-side (h_s) is estimated from the following:

$$h_s = \frac{0.36k_s}{D_e} \, \text{Re}_s^{0.55} \text{Pr}_s^{1/3}$$

$$for \; 2 \times 10^3 < \text{Re}_s = \frac{G_s D_e}{\mu_s} < 1 \times 10^6 \tag{58}$$

Where k_s is the thermal conductivity of the shell-side fluid. The tube-side pressure drop is calculated by the following:

$$\Delta P = \frac{f_s G_s^2 (N_b + 1) D_s}{2\rho_s D_e \left(\frac{\mu_b}{\mu_{w,s}}\right)^{0.14}} \tag{59}$$

Where N_b is the number of baffles, ρ_s is the density of the shell-side fluid, μ_b is the viscosity of the shell-side fluid at bulk temperature, and $\mu_{w,s}$ is the viscosity of the tube-side fluid at wall temperature. The f_s is the friction factor for the shell and can be obtained as follows:

$$f_s = \exp\left[0.576 - 0.19 \ln\left(\text{Re}_s\right)\right] \; ; \; for \; 400, \text{Re}_s < 1 \times 10^6 \tag{60}$$

The wall temperature can be calculated as follows:

$$T_w = \frac{1}{2}\left(\frac{T_{H,in} + T_{H,out}}{2} + \frac{T_{C,in} + T_{C,out}}{2}\right) \tag{61}$$

According to Eq. (21), the heat transfer surface area (A) of the shell and tube heat exchanger is obtained by the following:

$$A = \frac{Q}{U_m F \Delta T_{LMTD}} \tag{62}$$

The required length of the heat exchanger can be calculated based on the heat transfer surface area as follows:

$$L = \frac{A}{\pi d_o N_t} \tag{63}$$

5. Optimization of heat exchangers

The applications of heat exchangers are very different. Therefore, they are optimized based on their application. The most common criteria for optimizing heat exchangers are the minimum initial cost, minimum operating cost, maximum effectiveness, minimum pressure drop, minimum heat transfer area, minimum weight or material, etc. These criteria can be optimized individually or in combination. It is clear from the above that the optimal design of heat exchangers is based on many geometrical and operational parameters with high complexity. So it is difficult to design a cheap and effective heat exchanger. The optimization techniques are usually applied to ensure the best performance as well as lower the cost of the heat exchanger. The optimization is carried out using different techniques. Traditional techniques such as linear and dynamic programming as well as

steepest descent usually fail to solve nonlinear large-scale problems. The need for gradient information is another drawback of traditional techniques. Therefore, it is not possible to solve non-differentiable functions using these methods. To overcome these difficulties, advanced optimization algorithms are developed which are gradient-free. Several advanced optimization methods, such as genetic algorithm (GA) [21], non-nominated sorting GA (NSGA-II) [22], bio-geography-based optimization (BBO) [23], particle swarm optimization (PSO) [24], Jaya algorithm, and teaching–learning-based optimization (TLBO) [25], had been used for the optimization of heat exchangers by many researchers each of which has its advantages and disadvantages. Using GA, it is possible to solve all optimization problems, which can be described with the chromosome encoding and solves problems with multiple solutions. But in order to use GA, it is necessary to set a number of specific algorithmic parameters such as jump probability, selection operator, cross probability. NSGA-II has an explicit diversity preservation mechanism and elitism prevents an already found Pareto optimal solution from being removed, but crowded comparison can limit the convergence and it needs the tuning of algorithmic-specific parameters including mutation probability, cross-over probability, etc. The optimization using BBO is also effective and it inhibits the degradation of the solutions, but poor exploiting the solutions is the main drawback of this method. The PSO is a heuristic and derivative-free technique that has the character of memory but it needs the tuning of algorithmic specific parameters and plurality of the population is not enough to achieve the global optimal solution. Similarly, TLBO and Jaya need the tuning of their own algorithmic-specific parameters [26].

Generally, an optimization design starts by selecting criteria (quantitatively) to minimize or maximize, which is called an objective function. In an optimization design, the requirements of a particular design such as required heat transfer, allowable pressure drop, limitations on height, width and/or length of the exchanger are called constraints. Several design variables such as operating mass flow rates and operating temperatures can also participate in an optimization design [15]. The single target optimization can be expressed as [27]:

$$\begin{aligned} \min \ & f(x) \\ & g_i(x) \geq 0, \ j = 1, \ 2, \ \ldots, \ J \\ & h_k(x) \geq 0, \ k = 1, \ 2, \ \ldots, \ K \end{aligned} \tag{64}$$

Where $f(x)$ is the objective function, $g_i(x) \geq 0$ is the inequality constraint, and $h_i(x) \geq 0$ is the equality constraint. Multi-objective combination optimization can be indicated as [27]:

$$\begin{aligned} \min \ & f(x) = \big(f_1(x), \ f_2(x), \ \ldots, f_m(x) \big) \\ & g_i(x) \geq 0, \ j = 1, \ 2, \ \ldots, \ J \\ & h_k(x) \geq 0, \ k = 1, \ 2, \ \ldots, \ K \end{aligned} \tag{65}$$

Using the data modeling, the optimization of a heat exchanger can be transformed into a constrained optimization problem and then solved by modern optimization algorithms. In this chapter, the focus is on GA and PSO because many researchers mentioned that these algorithms lead to remarkable savings in computational time and have an advantage over other methods in obtaining multiple solutions of the same quality. So it gives more flexibility to the designer [2].

5.1 Genetic algorithm

GA is a search heuristic that is inspired by Charles Darwin's theory of survival of the fittest, which explains inferior creatures pass away and superior creatures remain [28]. In GA, sets of design variables are codified by sequences with fixed or variable lengths, similar to chromosomes or individuals in biological systems. Each chromosome is formed of several design variables, which are known as genes. In repetitive processes such as GA, each repetitive stage is a generation and a collection of solutions associated with each generation is a population. Generally, the initial population is generated randomly [29]. In GA statistical methods are used to achieve optimum points. In the process of natural selection, populations are selected based on their fitness. A new population is formed using genetic operations containing selection, crossover, mutation, etc. This cycle continues until a certain result is achieved or the stop criterion is satisfied [30]. **Figure 7** shows the flowchart of GA and the steps of binary GA are discussed below [32].

Step 1: Initialization of population

The initial population of GA includes binary numbers generated randomly which are chromosomes or GA strings, consisting of bits called genes. Actually, the initial population is the probable solution to the optimization problem. The number of gens (n_g) assigned to represent a variable in the chromosome depends on the precision ϵ and the range of the variable [x_{min}, x_{max}], and is given by

$$n_g = \log_2\left(\frac{x_{\min} - x_{\max}}{\epsilon}\right) \qquad (66)$$

Step 2: Fitness evaluation

The fitness value of each GA string is examined by first determining the decoded values of the variables D, and next the corresponding real values are obtained as follows:

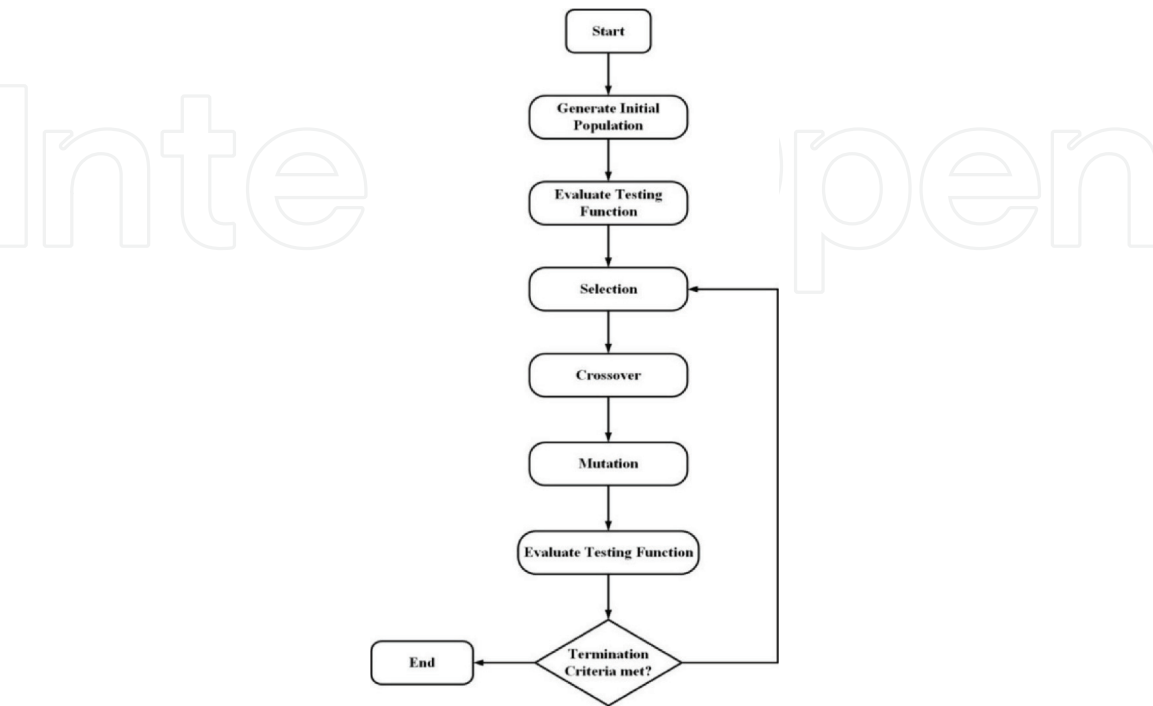$$x = x_{\min} + \frac{x_{\max} - x_{\min}}{2^{n_g} - 1} \qquad (67)$$

Figure 7.
Flow chart of GA [31].

The fitness function values are then computed knowing the real values of design variables.

Step 3: Reproduction/selection

In this step, chromosomes with better fitness values to participate in the crossover are selected. Several selection modes such as roulette wheel selection or proportionate selection, rank-based selection, and tournament selection can be used in this step [33]. In proportionate selection, the probability of a chromosome to be selected is directly proportional to its fitness value. Hence, the chromosome having a better fitness value has a higher chance of selection for reproduction. This may result in premature convergence of the solution because there is a chance of losing diversity. The tournament selection is faster compared with the other two selection methods. In this method, n chromosomes are randomly picked from the population of solutions, where n represents the tournament size. The chromosome having the best fitness value is copied to the mating pool and all the n GA strings are returned to the population. This process is repeated for obtaining all the individuals of the mating pool.

Step 4: Crossover

The genes are exchanged between two-parent chromosomes in the crossover step, which leads to a new set of solutions, called children. The crossover operation represents the selection pressure or exploitation of fit chromosomes for even better solutions. The crossover probability (P_c) specifies the number of individuals taking part in the crossover operation, and this control parameter value is optimally chosen as nearly equal to 1.0. Several schemes of crossover such as single-point crossover, two-point crossover, multipoint crossover, and uniform crossover can be used in this step. A comparison of these methods is given in the literature [34].

Step 5: Mutation

Mutation means the change of a bit from 0 to 1 and from 1 to 0 in the solution chromosome, which is used for the exploration of new solutions. It helps to come out of the local basin and search for a global solution. The mutation probability P_m specifies the number of mutations and is commonly kept very low. Because if its value is high, the qualified solutions may be lost. The range of P_m is given as

$$\frac{0.1}{l} \leq P_m \leq \frac{1}{l} \tag{68}$$

Where l represents the length of the GA string. Steps 2, 3, 4, and 5 are repeated until the termination criterion (maximum number of generations or desired precision of solution) is met.

5.2 Particle swarm optimization

The PSO is inspired by the way fish and birds swarm search for food [35]. In this method, each particle represents one solution to a problem and they aim to find optimum points in a search space. This method is also based on the behavior of birds that they use to find their orientation. Based on this direction, the collective location of the swarm and the best individual location of particles per time are calculated and a new search orientation is composed of these two orientations and the previous orientation. In a search space of the D dimension, the best individual location of a particle and the best location of the overall particle are defined as Eqs. (69) and (70), respectively.

$$\vec{P}_1 = C_1\left(\vec{P}_{i1},\ \vec{P}_{i2},\ \ldots,\ \vec{P}_{iD}\right) \tag{69}$$

$$\vec{g}_1 = C_1\left(\vec{g}_1, \ \vec{g}_2, \ \ldots, \ \vec{g}_D\right) \tag{70}$$

The best location in the vicinity of each particle is given as below:

$$\vec{n} = \left(\vec{n}_{i1}, \ \vec{n}_{i2}, \ \ldots, \ \vec{n}_{iD}\right) \tag{71}$$

Displacement of particles after determination their velocity is as follows:

$$\vec{x}(t) = \vec{x}(t-1) + \vec{v}(t) \tag{72}$$

$$\vec{v}(t) = \vec{v}(t-1) + \vec{F}(t-1) \tag{73}$$

The best individual location of the particle and the best collective location of particles as two springs connected to the particle are used to model the force entered in the particle. The first spring is directed to the best individual experience and the second spring is directed to the best swarm experience. Eq. (74) shows the force entered in the particle.

$$\vec{F}_{i-1} = C_1\left(\vec{P}_{i-1} - \vec{x}_{i-1}\right) + C_2\left(\vec{g}_{i-1} - \vec{x}_{i-1}\right) \tag{74}$$

Where C_1 and C_2 are acceleration coefficients. The particle velocity at dimension d (v_{id}) and the next repetition can be obtained as follows [35]:

$$\begin{aligned} v_{id}(t) = \omega v_{id}(t-1) + C_1 rand_1(P_{id}(t-1) - x_{id}(t-1)) \\ + C_2 rand_2(n_{id}(t-1) - x_{id}(t-1)) \end{aligned} \tag{75}$$

This shows the velocity of particle i at the star topology or global best. The rand$_1$ and rand$_2$ are random numbers that have a constant distribution in the range 0–1. **Figure 8** shows the flowchart of PSO and the steps of PSO are discussed below [32].
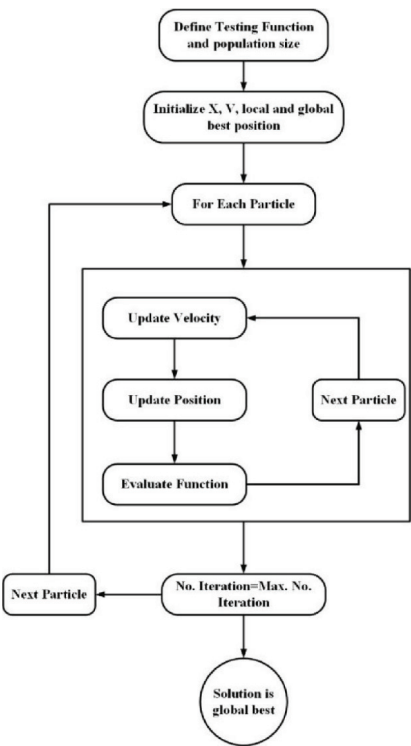

Figure 8.
Flow chart of PSO [31].

Step 1: Initialization

The swarm of potential solutions is generated with random positions and velocities. The i*th* particle in D-dimensional space may be denoted as $X_i = (x_{i1}, x_{i2}, ..., x_{id})$ and $i = 1, 2,..., N$, where N denotes the size of the swarm.

Step 2: Fitness evaluation

The corresponding fitness values of the particles are evaluated.

Step 3: Determination of personal and global best

The best individual location of a particle ($\vec{P}_1$) is sorted, the particle having the best fitness value is determined for the current generation, and the best location ($\vec{g}_1$) is updated.

Step 4: Velocity and position update

The velocity and position of the ith particle are updated based on Eq. (75).

Here, an example of the design and optimization of a shell and tube heat exchanger is presented. This example was used by Karimi et al. (2021) [36]. Their aim was to minimize the total annual cost (C_{tot}) for a shell and tube heat exchanger based on optimization algorithms. The total annual cost is the sum of the initial cost for the construction (C_i) of the heat exchanger and the cost of power consumption in the shell and tube heat exchanger (C_{od}). Hence, the total annual cost was considered as an objective function that should be minimized using GA and PSO. Process input data and physical properties for this case study are presented in **Table 4**. Also, bounds for design parameters are listed in **Table 5**. The objective function can be written as follows:

$$C_{tot} = C_i + C_{od} \qquad (76)$$

The results show that the use of PSO has been led to lower Ctot, which means that the minimization of cost function was performed better using this algorithm. Also, the use of PSO resulted in lower Δp and A as well as higher U (**Table 6**).

	$\dot{m}$ $\left(\dfrac{\text{kg}}{s}\right)$	T_{in} (°C)	T_{out} (°C)	ρ $\left(\dfrac{\text{kg}}{m^3}\right)$	C_p $\left(\dfrac{J}{\text{kg}}\right)$	μ (Pas)	k $\left(\dfrac{W}{m.K}\right)$	R_f $\left(\dfrac{m^2 K}{W}\right)$	μ_w (Pas)
Shell side: methanol	27.8	95	40	750	2840	0.00034	0.19	0.00033	0.00038
Tube side: sea water	68.9	25	40	995	4200	0.0008	0.59	0.0002	0.00052

Table 4.
Process input data and physical properties for three case studies [36].

Parameters	Lower value	Upper value
Tubes outside diameters(m)	0.015	0.051
Shell diameters(m)	0.1	1.5
Central baffle spacing(m)	0.05	0.5

Table 5.
Bounds for design parameters [36].

	PSO	GA
$L\ (m)$	2.6871	3.9089
$d_o\ (m)$	0.015063	0.015
$B\ (m)$	0.49967	0.49989
$D_s\ (m)$	0.81143	0.74105
$N_t\ (m)$	1238	1365.5
$\nu_t\ (m/s)$	0.83349	0.893
Re_t	27,909	13,386
Pr_t	5.69	5.69
$h_t\ (W/m^2K)$	3740.8	4639.7
f_t	0.0212	0.0073
$\Delta P_t\ (Pa)$	4730	5191.3
$D_e\ (m)$	0.0141	0.0106
$\nu_s\ (m/s)$	0.498	0.499
Re_s	15,489	11,716
Pr_s	5.1	5.1
$h_s\ (W/m^2K)$	9075.7	1648.9
f_s	0.313	0.353
$\Delta P_s\ (Pa)$	21,355	18,033
$U\ (W/m^2K)$	900.98	686.71
$A\ (m^2)$	198.78	252.58
$C_i\ (\$)$	44,116	50,737
$C_o\ (\$)$	2561.5	1085.2
$C_{od}\ (\$)$	2340	6685
$C_{tot}\ (\$)$	46,456	57422.51

Table 6.
Optimal parameter of heat exchanger using GA and PSO algorithms [36].

6. Conclusion

This chapter has discussed the thermal design and optimization of shell and tube heat exchangers. The basic equations of heat transfer were investigated and log-mean temperature difference (LMTD) and effectiveness-number of transfer units (ε-NTU) were presented. The thermal design was focused on Kern's method. In this method, it is assumed the shell flow is ideal, and leakage and bypass are negligible. Based on this flow model, only a single stream flows in the shell that is driven by baffles. This can lead to a very simple and rapid calculation of shell-side coefficients and pressure drop. The optimization of heat exchangers is presented based on the genetic algorithm (GA) and particle swarm optimization (PSO) due to the recommendation of these methods by man researchers because of quick convergence and obtaining multiple solutions.

Conflict of interest

The authors declare no conflict of interest.

Nomenclature

A	*Total heat transfer area*
A_s	*Cross-flow area at the shell diameter*
B	*Baffle spacing*
Cp	*Heat capacity*
C_i	*Capital investment cost*
C_o	*Total operating cost*
C_{od}	*Total discounted operating cost*
C_r	*Capacity ratio*
C_t	*Clearance between adjacent tubes*
C_{tot}	*Total annual cost*
CL	*Tube layout constant*
CTP	*Tube count calculation constant*
d_w	*Wall thickness*
D_s	*Shell diameter*
F_s	*Friction factor for shell*
G_s	*Mass flow rate of shell-side fluid*
h	*Convection heat transfer coefficient*
k	*Thermal conductivity*
K	*Heat conductivity coefficient*
L	*Tube length*
$LMTD$	*Logarithmic mean temperature difference*
$\dot{m}_s$	*Flow rate of shell-side fluid*
N_t	*Number of tubes*
NTU	Number of heat transfer unit
P	*Thermal effectiveness*
P_r	*Tube pitch ratio*
P_t	*Tube pitch constant*
Pr	*Prandtl number*
q	*Actual heat transfer rate*
q_{max}	*Maximum possible heat transfer rate*
Q	*Heat transfer rate*
r_i	*Inside diameter*
r_o	*Outside diameter*
R	*Thermal resistance*
Re	*Reynolds number*
T	*Temperature*
U	*Overall heat transfer coefficient*
U_m	*Mean overall heat transfer coefficient*

Greek symbols

Δ	Difference
ε	*Effectiveness*
ρ	*Density*
μ	*Dynamic viscosity*
ν	**Velocity**

Subscripts

b	*Bulk*
C	*Cold*

c	*Convection*
H	*Cold*
i	*Inside*
max	*Maximum*
min	*Minimum*
o	*Outside*
s	*Shell side*
t	*Tube side*

Author details

Shahin Kharaji
Research and Develop Department, FAPKCO Engineering Group, Shiraz, Iran

*Address all correspondence to: shahinkharaji@gmail.com

IntechOpen

References

[1] Ghalandari, M., et al., Applications of intelligent methods in various types of heat exchangers: a review. Journal of Thermal Analysis and Calorimetry, 2021. 145(4): p. 1837-1848

[2] Lahiri SK, Khalfe NM, Wadhwa SK. Particle swarm optimization technique for the optimal design of shell and tube heat exchangers. Chemical Product and Process Modeling. 2012;7(1), Article 14.

[3] Ezgi CN. Basic Design Methods of Heat Exchanger. In: Heat Exchangers-Design, Experiment and Simulation. Rijeka: IntechOpen; 2017

[4] Chen Q, Ren J. Generalized thermal resistance for convective heat transfer and its relation to entransy dissipation. Chinese Science Bulletin. 2008;53(23): 3753-3761

[5] Marner W, Suitor J. Survey of Gas-Side Fouling in Industrial Heat-Transfer Equipment. Final Report. Pasadena, CA (USA): Jet Propulsion Lab; 1983

[6] Whitaker S. Fundamental Principles of Heat Transfer. Oxford, United kingdom: Pergamon press, Elsevier; 2013

[7] Çengel YA, Ghajar AJ. Heat and Mass Transfer: Fundamentals [and] Applications. New York City, United States: McGraw-Hill Education; 2020

[8] Borjigin S et al. Coupling ε-NTU method for thermal design of heat exchanger in cabinet cooling system. Applied Thermal Engineering. 2019;159: 113972

[9] Smith R. Chemical Process Design And Integration. New York City, United States: John Wiley & Sons; 2005

[10] Vengateson U. Design of multiple shell and tube heat exchangers in series: E shell and F shell. Chemical Engineering Research and Design. 2010;88(5–6): 725-736

[11] Wales, R. and W. RE, Mean Temperature Difference in Heat Exchangers. New York, United state Chemical Engineering Journal; 1981

[12] Fakheri A. Log mean temperature correction factor: an alternative representation. In: Proceedings of the International Mechanical Engineering Congress and Exposition. New Orleans, Louisiana: Citeseer; 2002

[13] Gulyani BB, Jain A, Kumar S. Optimal synthesis of multipass heat exchanger without resorting to correction factor. International Journal of Mechanical, Aerospace, Industrial, Mechatronic and Manufacturing Engineering. 2011;5(5):898-904

[14] Iu I et al. Applying the effectiveness-NTU method to elemental heat exchanger models. ASHRAE Transactions. 2007;113(1):504-513

[15] Shah RK, Sekulic DP. Fundamentals of Heat Exchanger Design. New York City, United States: John Wiley & Sons; 2003

[16] Silaipillayarputhur K, Khurshid H. The design of shell and tube heat exchangers–A review. International Journal of Mechanical and Production Engineering Research and Development. 2019;9(1):87-102

[17] Alperen MA, Kayabaşi E, Kurt H. Detailed comparison of the methods used in the heat transfer coefficient and pressure loss calculation of shell side of shell and tube heat exchangers with the experimental results. Energy Sources, Part A: Recovery, Utilization, and Environmental Effects. 2019:1-20

[18] Standard I. Specification for Shell and Tube Type Heat Exchangers. New Delhi: BIS 2007; 2007

[19] Jalilirad S, Cheraghali MH, Ashtiani HAD. Optimal design of shell-

and-tube heat exchanger based on particle swarm optimization technique. Journal of Computational Applied Mechanics. 2015;**46**(1):21-29

[20] Anescu, G., A DMSACO Approach to Economic Heat Exchanger Design. Politechnica University of Bucharest in Romania.

[21] Guo J, Cheng L, Xu M. Optimization design of shell-and-tube heat exchanger by entropy generation minimization and genetic algorithm. Applied Thermal Engineering. 2009;**29**(14–15):2954-2960

[22] Yin Q et al. Optimization design and economic analyses of heat recovery exchangers on rotary kilns. Applied Energy. 2016;**180**:743-756

[23] Hadidi A, Nazari A. Design and economic optimization of shell-and-tube heat exchangers using biogeography-based (BBO) algorithm. Applied Thermal Engineering. 2013;**51**(1–2):1263-1272

[24] Patel V, Rao R. Design optimization of shell-and-tube heat exchanger using particle swarm optimization technique. Applied Thermal Engineering. 2010;**30**(11–12):1417-1425

[25] Rao RV, Patel V. Multi-objective optimization of heat exchangers using a modified teaching-learning-based optimization algorithm. Applied Mathematical Modelling. 2013;**37**(3):1147-1162

[26] Rao RV et al. Design optimization of heat exchangers with advanced optimization techniques: A review. Archives of Computational Methods in Engineering. 2020;**27**(2):517-548

[27] Yao J. A review of industrial heat exchange optimization. In: IOP Conference Series: Earth and Environmental Science. JIOP Publishing Ltd in Bristol, England; 2018

[28] Haupt RL, Haupt SE. Practical Genetic Algorithms. New York City, United States: John Wiley & Sons; 2004

[29] Najafi H, Najafi B, Hoseinpoori P. Energy and cost optimization of a plate and fin heat exchanger using genetic algorithm. Applied Thermal Engineering. 2011;**31**(10):1839-1847

[30] Konak A, Coit DW, Smith AE. Multi-objective optimization using genetic algorithms: A tutorial. Reliability Engineering & System Safety. 2006;**91**(9):992-1007

[31] Sadeghzadeh H, Ehyaei M, Rosen M. Techno-economic optimization of a shell and tube heat exchanger by genetic and particle swarm algorithms. Energy Conversion and Management. 2015;**93**:84-91

[32] Swayamsiddha S. Bio-inspired algorithms: principles, implementation, and applications to wireless communication. In: Nature-Inspired Computation and Swarm Intelligence. Cambridge, Massachusetts, United States: Academic Press; 2020. pp. 49-63

[33] Blickle T, Thiele L. A Comparison of Selection Schemes used in Genetic Algorithms, TIK-Report No. 11. Computer Engineering and Communication Networks Lab (TIK) Zurich, Switzerland; 1995

[34] Spears WM, Anand V. A study of crossover operators in genetic programming. In: International Symposium on Methodologies for Intelligent Systems. Berlin, Heidelberg: Springer; 1991

[35] Shi Y. Particle swarm optimization: developments, applications and resources. In: Proceedings of the 2001 Congress on Evolutionary Computation (IEEE Cat. No. 01TH8546). Seoul, Korea (South); 2001

[36] Karimi, H., H. Ahmadi Danesh Ashtiani, and C. Aghanajafi, Optimization Techniques for Design a shell and tube heat exchanger from economic view. AUT Journal of Mechanical Engineering, 2021. **5**(2): 9-9